Muon–fluorine entanglement in fluoropolymers

2009 J. Phys.: Condens. Matter 21 346004

(http://iopscience.iop.org/0953-8984/21/34/346004)

J. Phys.: Condens. Matter **21** (2009) 346004 (6pp) doi:10.1088/0953-8984/21/34/346004

Muon–fluorine entanglement in fluoropolymers

T Lancaster[1], F L Pratt[2], S J Blundell[1], I McKenzie[2] and H E Assender[3]

[1] Department of Physics, Clarendon Laboratory, Oxford University, Parks Road, Oxford OX1 3PU, UK
[2] ISIS Facility, Rutherford Appleton Laboratory, Chilton, Oxfordshire OX11 0QX, UK
[3] Department of Materials, Oxford University, Parks Road, Oxford OX1 3PH, UK

E-mail: t.lancaster1@physics.ox.ac.uk

Received 23 March 2009, in final form 14 July 2009
Published 5 August 2009
Online at stacks.iop.org/JPhysCM/21/346004

Abstract
We present the results of muon spin relaxation measurements on the fluoropolymers polytetrafluoroethylene (PTFE), poly(vinylidene fluoride) (PVDF) and poly(vinyl fluoride) (PVF). Entanglement between the muon spin and the spins of the fluorine nuclei in the polymers allows us to identify the different muon stopping states that occur in each of these materials and provides a method of probing the local environment of the muon and the dynamics of the polymer chains.

(Some figures in this article are in colour only in the electronic version)

1. Introduction

Muon spin relaxation (μ^+SR) may be used to investigate a range of physical behaviour in polymers including bulk and surface structural dynamics [1, 2] and the behaviour of mobile charge carriers [3]. Initial μ^+SR measurements on the fluorinated polymer poly(tetrafluoroethylene) (PTFE) showed that the majority of muons implanted in this system realized diamagnetic states where the muon spin became entangled with two fluorine nuclei [1, 4]. These states provide a sensitive means of probing the muons' local environment and characterizing the degree of distortion introduced by the presence of the charged muon probe. We therefore have the possibility that the electronegative fluorines in fluoropolymers can provide 'traps' for positive muons, so that the local physical properties in such systems can be probed from well characterized muon sites. Here we extend this investigation to the fluoropolymers poly(vinylidene fluoride) (PVDF) and poly(vinyl fluoride) (PVF). In each case we find that the muon enters a distinct stopping state characterized by a different degree of entanglement with the surrounding fluorines.

In a μ^+SR experiment, spin-polarized positive muons are stopped in a target sample and the time evolution of the muon ensemble spin polarization is observed [5]. Localized muons often interact with spins in their environment via dipole–dipole coupling described by the two-spin Hamiltonian

$$\mathcal{H} = \sum_{i>j} \frac{\mu_0 \gamma_i \gamma_j}{4\pi r^3} [\mathbf{S}_i \cdot \mathbf{S}_j - 3(\mathbf{S}_i \cdot \hat{\mathbf{r}})(\mathbf{S}_j \cdot \hat{\mathbf{r}})], \qquad (1)$$

where $\mathbf{r}$ is the vector linking spins S_i and S_j, which have gyromagnetic ratios $\gamma_{i,j}$. The observed property of the experiment, the polarization $D_z(t)$ of the muon ensemble along a quantization axis z, is given by [6]

$$D_z(t) = \frac{1}{N} \left\langle \sum_{m,n} |\langle m|\sigma_q|n\rangle|^2 \cos(\omega_{mn} t) \right\rangle_q, \qquad (2)$$

where N is the number of spins, $|m\rangle$ and $|n\rangle$ are eigenstates of the total Hamiltonian $\mathcal{H}$, σ_q is the Pauli spin matrix corresponding to the direction q and $\langle\rangle_q$ represents an appropriately weighted powder average[4].

In fluorinated materials, where the muon is preferentially drawn towards the electronegative fluorine atoms, the muon spin may interact strongly with a small number of fluorine spins via the Hamiltonian in equation (1). In the case of the alkali fluorides [7], for example, the muon and two fluorine

[4] The vibrational frequency of the muon–fluorine bond exceeds by orders of magnitude both the frequencies observable in a muSR experiment and the frequency appropriate to the dipolar coupling in equation (1); thus the bond length probed via these entangled states is time averaged over thermal fluctuations and yields a reliable estimate.

ions form a strong, linear 'hydrogen bond' [8] (the so-called F–μ^+–F state) usually separated by slightly less than twice the F^- ionic radius (2.66 Å). In chemically complex materials such as the molecular magnetic coordination polymers, other states may be formed, including interaction with a single F, and more complicated arrangements [9]. Each of these cases involves quantum entanglement, in that the state vector describing the composite system cannot be separated into a product of state vectors describing each spin system and that this non-separable state is needed to correctly reproduce the measured spectra. It should be noted, though, that the observation of these entangled states represents the exception, rather than the rule. In most materials the large number of spin centres surrounding the muon allows the use of the local magnetic field (LMF) approximation, where the muon spin S effectively interacts with the net local magnetic field $\langle B\rangle$ at its stopping site via the Hamiltonian $\mathcal{H} = \gamma_\mu S\langle B\rangle$, where γ_μ is the muon gyromagnetic ratio. For the commonly observed case of the muon response to an ensemble of randomized static local fields, the LMF model gives the Kubo–Toyabe (KT) function [10],

$$D_z(t) = \frac{1}{3} + \frac{2}{3}(1-\Delta^2t^2)\exp\left(-\frac{\Delta^2t^2}{2}\right), \tag{3}$$

where Δ is proportional to the second moment of the local magnetic field distribution. The 1/3 term is often not observed due to the presence of slow dynamics in the field distribution. The resulting relaxation which is observed is usually well approximated by a Gaussian function $\exp(-\sigma^2t^2)$ at early times.

Below we discuss the results of zero field (ZF) μ^+SR measurements on three fluorinated polymeric materials, namely PTFE, PVDF and PVF. ZF μ^+SR measurements were made on the ARGUS and MuSR instruments at the ISIS facility, Rutherford Appleton Laboratory, UK. Samples (obtained commercially) were mounted on a Ag backing plate in a helium flow cryostat or on the cold finger of a closed cycle refrigerator.

2. Results and discussion

2.1. PTFE

The PTFE chain $[–CF_2–CF_2–]_n$ is helical, with successive CF_2 units rotated slightly due to the steric interference of adjacent fluorine atoms [12]. PTFE is ≈50% crystalline and ≈50% amorphous and exists in multiple forms that are influenced by temperature, pressure and history. Since our experiments were made at ambient pressure and below 292 K, we are probing form II PTFE [12]. This form of PTFE (with unit cell parameters $a = 0.56, b = 0.56, c = 1.69$ nm) has a pseudohexagonal arrangement of chains in the a–b plane, with the helices repeating every 19.5 Å (15 CF_2 units) and no ordering in the c-axis.

Example ZF μ^+SR spectra for PTFE are shown in figure 1(a). Around a quarter of the expected initial asymmetry is missing due to the formation of muonium states [1], leaving the remaining three quarters in diamagnetic states which are sensitive to entanglement with fluorine nuclei. The entanglement signal is observed below 200 K and was described previously [1, 4] by a linear F–μ^+–F model which leads (in the absence of any external dipole–dipole interactions) to the polarization function [7]

$$\begin{aligned} D(\omega_i t) = \frac{1}{6}\Bigg[3 &+ \cos(\sqrt{3}\omega_i t) \\ &+ \left(1-\frac{1}{\sqrt{3}}\right)\cos\left[\left(\frac{3-\sqrt{3}}{2}\omega_i t\right)\right] \\ &+ \left(1+\frac{1}{\sqrt{3}}\right)\cos\left[\left(\frac{3+\sqrt{3}}{2}\omega_i t\right)\right]\Bigg], \end{aligned} \tag{4}$$

where $\omega_i = \mu_0\gamma_\mu\gamma_F/4\pi r_i^3$, γ_F is the ^{19}F nuclear gyromagnetic ratio and r_i is the μ^+–^{19}F separation. The energy level transitions giving rise to this function are shown in figure 1(b) We note that this analytical form neglects F–F nuclear coupling, which provides a small correction to the relaxation. The linear F–μ^+–F model accounts well for the μ^+SR signal observed in the alkali metal fluorides [7] and in other inorganic compounds (see e.g. [13].)

In contrast to the previous results [1, 4], our high-statistics measurements of the entanglement signal in PTFE suggest that it is best described by the sum of two linear F–μ–F signals with slightly different bond lengths r_i. The total muon ensemble response is best modelled by the sum of this F–μ^+–F contribution and a small contribution to the relaxation which has a Gaussian character. This latter contribution would appear to arise from muon sites which do not contribute to the entanglement signal, but which instead experience a random distribution of magnetic fields. As discussed above, this should give the KT function in the LMF approximation, but the presence of slow dynamics causes it to resemble the Gaussian contribution that we observe. Typical spectra were, therefore, fitted with the resulting relaxation function

$$\begin{aligned} A(t) = A_1 D_z(\omega_1 t)\exp(-\lambda_1 t) + A_2 D_z(\omega_2 t)\exp(-\lambda_2 t) \\ + A_3\exp(-\sigma^2t^2) + A_{bg}, \end{aligned} \tag{5}$$

where A_{bg} accounts for those muons that stop in the sample holder or cryostat tails. The exponential factors $\exp(-\lambda_i t)$ multiplying the entanglement signal crudely model slow dynamics in the F–μ–F state [10]. We note that a more accurate fitting model involving the dynamicization of the entanglement function (as described in [11]) did not lead to significantly different results. The fitted amplitudes at 20 K are found to be $A_1 = 5.08(8)$, $A_2 = 11.6(1)$ and $A_3 = 2.6(1)$%, demonstrating that the greater part of the relaxation arises from the entangled states. The Gaussian relaxation rate was found to be approximately temperature dependent at $\sigma = 0.35$ MHz.

At $T = 20$ K we obtain interaction frequencies $\omega_1 = 0.199(1)$ MHz and $\omega_2 = 0.181(1)$ MHz corresponding to F–μ^+ separations of $r_1 = 0.122(1)$ nm and $r_2 = 0.126(1)$ nm. With increasing T, each ω_i falls smoothly, with ω_2 falling more dramatically than ω_1 (figure 1(c)). Hydrogen bond lengths are known to be very sensitive to changes in temperature [14], which also seems to be true for the muon–fluorine bond in the F–μ^+–F state in PTFE. The weakness of these bonds implies that thermal and quantum mechanical effects determine the

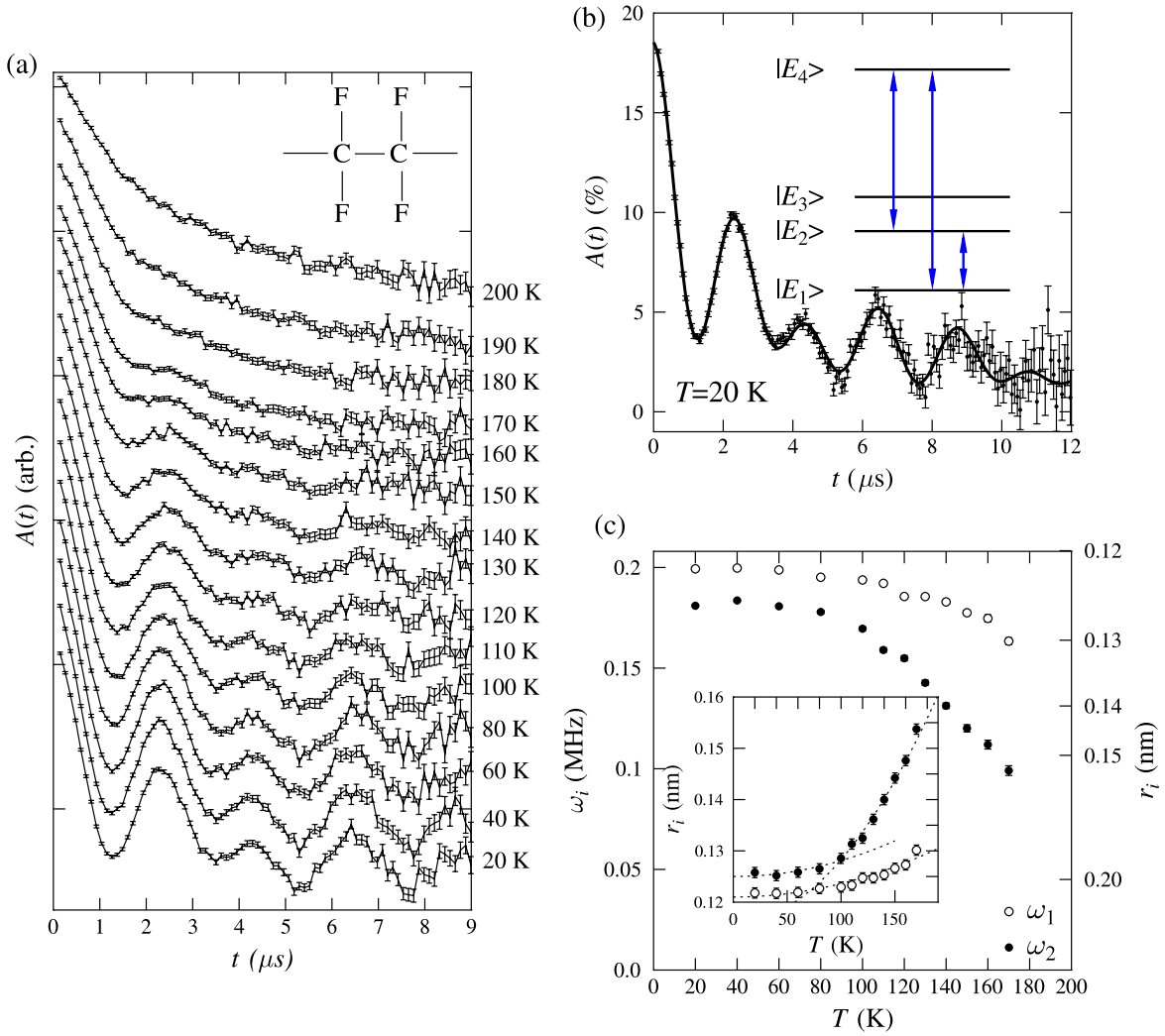

Figure 1. (a) Temperature evolution of the data measured on PTFE. (b) ZF μ^+SR spectra for PTFE measured at 20 K. The data is fitted to equation (5) which describes two linear F–μ^+–F signals whose energy level structure is shown inset. (c) Fitted frequencies ω_i and F–μ^+ bond lengths as a function of temperature. The dotted lines are a guide to the eye, illustrating T^2 scaling laws.

bond length rather than quantum effects alone [14]. The inset in figure 1(c) shows that the bond length r_1 roughly follows the expected quadratic variation with temperature [14], but that r_2 cannot be modelled by a single T^2 scaling, with a suggestion of a crossover in behaviour around 100 K (figure 1).

As observed previously [1], the spectra change their form above about 180 K, with the entangled state becoming unobservable above this temperature. As the temperature is increased A_2 falls most dramatically, accompanied by an increase of the Gaussian fraction with amplitude A_3 (figure 2(a)). The amplitude A_1 does not vary appreciably, and relaxation rates λ_1 and λ_2 increase with increasing temperature (figure 2(b)). Above 200 K the spectra are well described by exponential relaxation, typical of dynamic fluctuations in the local field distribution at the muon site [10]. We note that this crossover in the behaviour of the measured spectra around 200 K coincides with the PTFE glass II transition (occurring at $T_{\rm gII} = 193$ K), which is the temperature below which rotations about the C–C bond freeze.

The addition of three components in equation (5) implies that there are three classes of muon stopping state to be accounted for: the two distinct entanglement signals, where that with amplitude A_2 has the larger bond length and relaxation rate and the greatest variation of r with temperature; and also the KT/Gaussian signal (with amplitude A_3) arising from muons experiencing a quasistatic random distribution of magnetic fields. We may identify two classes of candidate muon site in PTFE: (i) between two fluorines on a single PTFE chain, where a muon will cause a small distortion to the conformation of the chain; (ii) between fluorines on adjacent PTFE chains, forming the F–μ^+–F state and causing a small local distortion of the chains in its vicinity. We might also expect the latter to have the longer bond length and the greater variation with temperature. One possible explanation of our data is, therefore, that the signal with amplitude A_1, with its small relaxation rate and near constant amplitude, arises from muons stopped between fluorines on a single chain. The components with amplitudes A_2 (entangled) and A_3 (Gaussian) might then arise from sites between chains.

Although we have the possibility of these stopping states occurring in both the amorphous and crystalline regions of the material, we note that the significant amplitude of our total

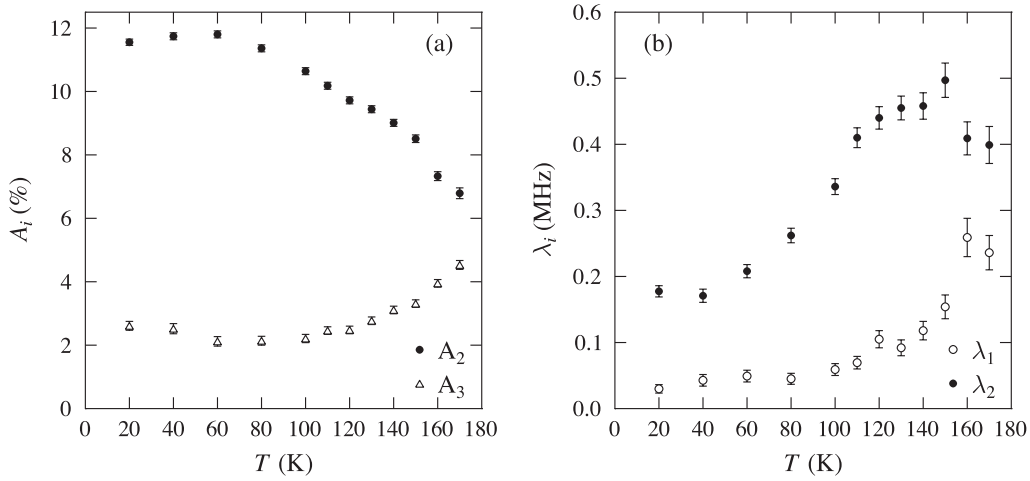

Figure 2. (a) Temperature evolution of the amplitudes A_2 (entangled) and A_3 (Gaussian) from equation (5). The Gaussian amplitude increases at the expense of the entangled amplitude as the temperature is increased. (b) Relaxation rates of the two entangled components showing an increase as temperature is increased.

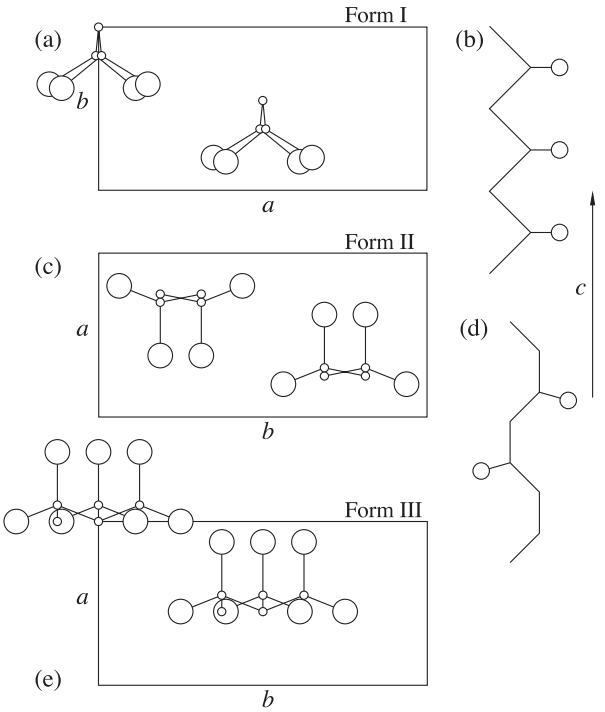

Figure 3. Structure of crystalline PVDF in each of its three phases [16]. Carbon is shown by small circles, fluorine by large circles. (a) and (b) Form I is a TT conformation; (c) and (d) form II has TGTG′ chains; (e) form III has TTTGTTTG′ chains.

entangled signal implies that the entangled states arise from muons stopping in both crystalline and amorphous regions. We do not, for example, obtain roughly equally weighted entangled and nonentangled signals, as might be expected for half of the muons stopping in each phase. This is reasonable, since we would expect the crystalline and amorphous regions to resemble each other at a local level. It is likely that the structure of the amorphous regions will still allow the F–μ^+–F states to form, but there is a greater relaxation from those states occurring between chains, due to the disorder in the surrounding fluorines. If this is indeed the case, then the μ^+–F separation in this component represents a weighted average of that in the crystalline and amorphous regions, which may account for its more dramatic variation with temperature. The states giving rise to the Gaussian component are likely to result mainly from stopping states where the local structure does not resemble the crystalline phase so closely and the muon is influenced by the local fields from many fluorine nuclear moments. As the temperature is increased these states are preferably formed, causing the amplitude of the Gaussian signal to increase at the expense of the interchain entangled fraction. Above the glass transition at T_{gII}, the F–μ^+–F bond made between fluorines on different chains will be continuously made and broken due to the rotational motion allowed above this temperature. This will wash out the coherent precession signal caused by the interchain entanglement. The increased dynamics above T_{gII} is also likely to be responsible for the increase in the relaxation rate λ_1 of the intrachain component. Taken together, this may account for the loss of the entanglement signal around 200 K.

2.2. PVDF

Like PTFE, PVDF $[–CH_2–CF_2–]_n$ is around 50% crystalline [15]. Three of its crystal phases are shown in figure 3: form I is an essentially planar zig-zag conformation (TT) with chains packed in the lattice so the dipoles (formed from the difference in electronegativity between fluorines and hydrogens) are parallel along the b axis on an orthorhombic lattice ($a = 0.86$, $b = 0.49$, $c = 0.26$ nm); form II has TGTG′ chains on a monoclinic lattice ($a = 0.50$, $b = 0.97$, $= 0.97$ nm); form III is polar with TTTGTTTG′ chains on an orthorhombic lattice ($a = 0.50$, $b = 0.96$, $= 0.46$ nm). Our sample is expected to contain a mixture of these crystalline phases.

An example spectrum measured on PVDF is shown in figure 4. In this case the entanglement signal is well described

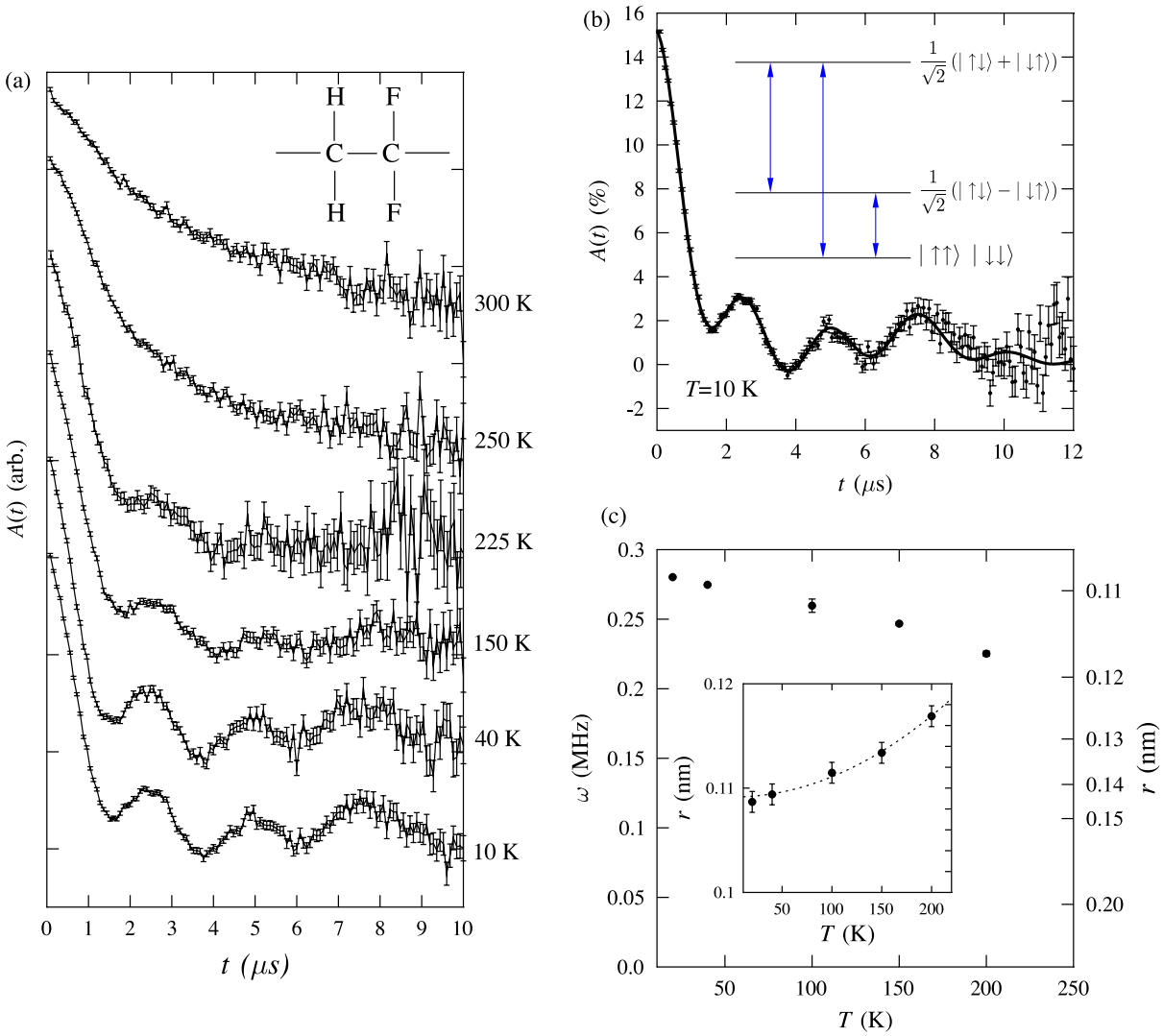

Figure 4. (a) Temperature evolution of the data measured on PVDF. (b) ZF μ^+SR spectra for PVDF measured at 10 K. The data is fitted to equation (5) describing a F–μ^+ model whose energy level structure is shown inset. (c) Fitted frequency ω_d and F–μ^+ bond length as a function of temperature. The dotted line shows a fit to a T^2 scaling law.

by the interaction of the muon with a single fluorine nucleus. This gives rise to a relaxation function

$$D_z(\omega t) = \frac{1}{6}\left[1+2\cos\left(\frac{\omega t}{2}\right)+\cos(\omega t)+2\cos\left(\frac{3\omega t}{2}\right)\right]. \quad (6)$$

The energy level transitions giving rise to this function are shown in figure 4(b). With this choice of $D_z(\omega t)$, the data may be fitted with equation (5). As in the case of PTFE, the signal is dominated by the component corresponding to the entanglement, with $A_1 = 10.3(2)\%$ and $A_2 = 2.7(2)\%$ at 10 K. Relaxation rates for PVDF were found to be $\lambda = 0.23(1)$ MHz and $\sigma = 0.19(3)$ MHz at 10 K, with both varying little across the temperature range. In this case we obtain a F–μ^+ separation of $r = 0.110(1)$ nm at 10 K. The bond length increases with increasing temperature (figure 4(c)), showing the expected quadratic variation with temperature. As the temperature is increased we again observe a crossover, with the amplitude in the Gaussian signal increasing with increasing temperature at the expense of the entangled fraction.

The reason for the occurrence of the F–μ^+ state, rather than the more commonly observed F–μ^+–F state, may be found in the crystal structures of PVDF [16] (figure 3). In each form of PVDF (figure 3), the crystal structure [16] is stabilized by the hydrogen atoms coordinating with the electronegative fluorines on adjacent chains. The possibility of a muon sitting between two fluorines does not, therefore, arise, as fluorines do not approach each other. Instead, the fluorines coordinate to hydrogen atoms. Muon sites then occur near the electronegative fluorine and try to avoid the hydrogen atoms. The relaxation of the F–μ^+ state will probably, therefore, be dominated by the disordered proton moments in the vicinity of the stopping sites.

As with PTFE, it is likely in this case that we are also probing both crystalline and amorphous phases. In the amorphous phases of PVDF we again might expect the arrangement of the chains to bear a similarity to the crystalline arrangement, with electronegative fluorines preferentially avoiding each other, preferring to orient themselves to the

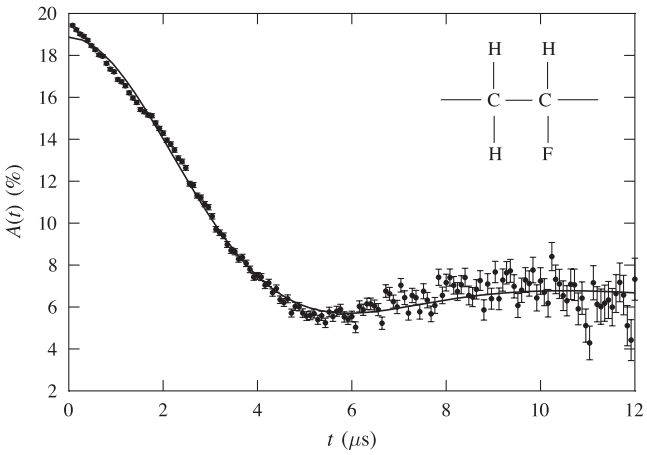

Figure 5. ZF μ^+SR spectrum measured at 10 K for PVF. The fit is to a dynamicized KT function.

more electropositive protonated side of the chain. The muons therefore still preferentially form F–μ^+ bonds but we might expect greater relaxation of the signal from those states in the amorphous regions.

2.3. PVF

PVF [–CH_2–CHF–]$_n$ is ≈40 % crystalline with chains forming a hexagonal lattice ($a = b = 0.49, c = 0.25$ nm) and has a glass transition temperature of 337 K [17].

A spectrum measured at 10 K for PVF is shown in figure 5. In contrast to the other two cases considered here, an entanglement signal cannot be resolved. Instead the spectra at all temperatures are quite well described by a KT function which arises due to the muon ensemble experiencing a random distribution of magnetic fields. The absence of the expected '1/3 tail' in the measured spectrum is attributable to slow dynamics in the local fields, which are also evident in the entangled signals. This may be modelled in the strong collision approximation [10] by a fluctuation rate ν. Fits to a dynamicized KT function at 10 K account for the full asymmetry amplitude of the signal and yield $\Delta = 0.330(2)$ MHz, $\nu = 0.120(1)$ MHz. As in the case of PVDF the fluorine atoms in adjacent chains will avoid approaching each other. It appears from our results that although it might be expected that muons will sit near the fluorines, the fact that there are several protons surrounding the muon provides enough static magnetic disorder to wash out the entanglement signal. This result is, however, surprising given the results on PVDF, where the local environment of the muon should be quite similar to this case.

3. Conclusion

In conclusion we have demonstrated the evolution of the nature of F–μ^+ entanglement in fluoropolymers. These results provide a demonstration that fluorinated materials allow the localization of muons in well defined stopping states where dipole interactions provide a quantum mechanical fingerprint that may be used to identify the state.

Acknowledgments

Part of this work was carried out at the ISIS facility, Rutherford Appleton Laboratory, UK. This work is supported by the EPSRC (UK). We are grateful to P Babkevich and W Hayes for useful discussions.

References

[1] Pratt F L, Blundell S J, Marshall I M, Lancaster T, Husmann A, Steer C, Hayes W, Fishmeister C, Martin R E and Holmes A B 2003 *Physica* B **326** 34
[2] Pratt F L, Lancaster T, Brooks M L, Blundell S J, Proksha T, Morenzoni E, Suter A, Leutkens H, Khasanov R, Scheuermann R, Shinotsuka K and Assender H E 2004 *Phys. Rev.* B **72** 121401
[3] Pratt F L, Blundell S J, Hayes W, Nagamine K, Ishida K and Monkman A P 1997 *Phys. Rev. Lett.* **79** 2855
[4] Nishiyama K, Nishiyama S W and Higetmoto W 2003 *Physica* B **326** 41
[5] Blundell S J 1999 *Contemp. Phys.* **40** 175
[6] Roduner E and Fischer H 1981 *Chem. Phys.* **54** 261
[7] Brewer J H, Kreitzman S R, Noakes D R, Ansaldo E J, Harshman D R and Keitel R 1986 *Phys. Rev.* B **33** 7813
[8] Emsley J 1980 *Chem. Soc. Rev.* **9** 91
[9] Lancaster T, Blundell S J, Baker P J, Brooks M L, Hayes W, Pratt F L, Manson J L and Schlueter J A 2007 *Phys. Rev. Lett.* **99** 267601
[10] Hayano R S, Uemura Y J, Imazato J, Nishida N, Yamazaki T and Kubo R 1979 *Phys. Rev.* B **20** 850
[11] Brewer J H, Harshman D R, Keitel R, Kreitzman S R, Luke G M, Noakes D R, Turner R E and Ansaldo E J 1986 *Hyperfine Interact.* **32** 677
[12] Kerbow D L 1989 *Polymer Handbook* 3rd edn, ed J Brandrup and E H Immergut (New York: Wiley) p 842 and references therein
[13] Lancaster T, Blundell S J, Baker P J, Hayes W, Giblin S R, McLain S E, Pratt F L, Salman Z, Jacobs E A, Turner J F C and Barnes T 2007 *Phys. Rev.* B **75** 220408R
[14] Dougherty R C 1998 *J. Chem. Phys.* **109** 7372
[15] Scheinbeim J I 1989 *Polymer Handbook* 3rd edn, ed J Brandrup and E H Immergut (New York: Wiley) p 949 and references therein
[16] Tadokoro H 1984 *Polymer* **25** 147
[17] Uschold R E 1989 *Polymer Handbook* 3rd edn, ed J Brandrup and E H Immergut (New York: Wiley) p 940 and references therein